

# A Final Word on FCNC-Baryogenesis from Heavy Higgs Bosons

Wei-Shu Hou<sup>1</sup>, Tanmoy Modak<sup>2</sup>, and Tilman Plehn<sup>2</sup>

<sup>1</sup> Department of Physics, National Taiwan University, Taipei, Taiwan

<sup>2</sup> Institut für Theoretische Physik, Universität Heidelberg, Germany  
modak@thphys.uni-heidelberg.de

December 16, 2020

## Abstract

Electroweak baryogenesis in a two-Higgs doublet model is a well-motivated and testable scenario for physics beyond the Standard Model. An attractive way of providing  $CP$  violation is through flavor-changing Higgs couplings, where linking top and charm quarks is hardly constrained by flavor and  $CP$ -violation constraints. We show how this scenario can be conclusively tested by searching for heavy charged and neutral Higgs bosons at the LHC. While the charged Higgs signature requires a dedicated analysis, the neutral Higgs signature will be covered by a general search for same-sign top pairs.

---

## Content

1	Introduction	2
2	Model and parameter space	2
3	Charged Higgs production	4
4	Neutral Higgs production	7
5	Outlook	9
A	Same-sign top study	10
	References	10

---

## 1 Introduction

The Higgs discovery [1,2] and subsequent measurements of the Higgs couplings [3–5] indicate that the Standard Model is the correct effective theory around the electroweak scale. While there exists no experimental evidence for physics beyond the Standard Model so far, extended Higgs sectors are motivated by theoretical considerations, like mass generation of up-type and down-type fermions, neutrino mass generation, electroweak baryogenesis, or dark matter. In particular, two-Higgs doublet models (2HDMs) [6–8] are an integral part of well-defined models for physics beyond the Standard Model, including MSSM [9], composite Higgs models [10], little Higgs models [11,12], or GUTs [13–16].

From an electroweak baryogenesis point of view [17], a 2HDM can provide both new scalar degrees of freedom [18,19] and  $CP$ -violation. In the general [20,21] or type-III [22] model, the additional states can be close in mass to the SM-Higgs [23,24]. Starting with two doublets, both coupling to up-type and down-type quarks hence two separate Yukawa matrices, we diagonalize the quark mass matrices and find the real, diagonal coupling  $\lambda_{ii} = \sqrt{2}m_i/v$  and the complex, non-diagonal coupling  $\rho_{ij}$ . Flavor-changing neutral couplings are generally constrained, but it is possible to have electroweak baryogenesis (EWBG) driven by an order-one, complex coupling  $\rho_{tc}$ . A valid parameter region is [25]

$$\text{Im } \rho_{tc} \gtrsim 0.5 \quad \text{and} \quad |\cos \gamma| \gtrsim 0.1, \quad (1)$$

where  $\gamma$  is the mixing angle between the two  $CP$ -even Higgs states.

A promising LHC search channel to test this kind of model is  $b$ -associated charged Higgs production [26]

$$cg \rightarrow bH^+ \rightarrow b(W^+h), \quad (2)$$

where the production process is induced by  $\rho_{tc}$  [27,28], while the decay amplitude is proportional to the mixing angle  $\cos \gamma$ . A sufficiently sensitive LHC search could therefore probe precisely the  $\rho_{tc}$ -EWBG scenario. In case the mixing angle  $\cos \gamma$  becomes small, the neutral Higgs production process

$$cg \rightarrow tA/H \rightarrow t(t\bar{c}), \quad (3)$$

with its same-sign top signature [29–33], provides a complementary probe for  $\rho_{tc}$ . In this paper we show how the LHC can conclusively probe the allowed parameter region of this model with the combination of heavy charged and neutral Higgs searches.

The paper is organized as follows: in Sec. 2 we discuss the model and its preferred parameter space, and then compare it to the reach of the charged Higgs channel in Sec. 3. Section 4 is dedicated to same-sign top production from neutral Higgs production and its complementarity to the charged Higgs signature. We summarize our results in Sec. 5.

## 2 Model and parameter space

The general  $CP$ -conserving two Higgs doublet potential can be written as [34,35]

$$\begin{aligned} V(\Phi, \Phi') = & \mu_{11}^2 |\Phi|^2 + \mu_{22}^2 |\Phi'|^2 - \left( \mu_{12}^2 \Phi^\dagger \Phi' + \text{h.c.} \right) + \frac{\eta_1}{2} |\Phi|^4 + \frac{\eta_2}{2} |\Phi'|^4 + \eta_3 |\Phi|^2 |\Phi'|^2 \\ & + \eta_4 |\Phi^\dagger \Phi'|^2 + \left[ \frac{\eta_5}{2} (\Phi^\dagger \Phi')^2 + (\eta_6 |\Phi|^2 + \eta_7 |\Phi'|^2) \Phi^\dagger \Phi' + \text{h.c.} \right]. \end{aligned} \quad (4)$$

In the Higgs basis, the VEV  $v = 246$  GeV is generated by the doublet  $\Phi$ , while  $\Phi'$  does not develop a VEV, hence  $\mu_{22}^2 > 0$ . The minimization conditions in the two field directions lead to  $\mu_{11}^2 = -\eta_1 v^2/2$  and  $\mu_{12}^2 = \eta_6 v^2/2$ . The mixing angle  $\gamma$  diagonalizes the  $CP$ -even mass matrix to define the mass eigenstates  $h$  and  $H$  [34, 35], satisfying the relations

$$c_\gamma^2 = \cos^2 \gamma = \frac{\eta_1 v^2 - m_h^2}{m_H^2 - m_h^2} \quad \text{and} \quad s_{2\gamma} = \sin(2\gamma) = \frac{2\eta_6 v^2}{m_H^2 - m_h^2} \quad (5)$$

simultaneously, where  $c_\gamma \rightarrow 0$  in the alignment limit ( $\eta_6 = 0$  and  $\eta_1 = m_h^2/v^2 \sim 1/4$ ). As one of the ingredients to baryogenesis, a strong first-order phase transition can be triggered by a second scalar degree of freedom close in mass with the SM-Higgs [36–38]. From Eq.(5) we see that this is guaranteed by finite  $c_\gamma$  and perturbatively stable  $\eta_i = \mathcal{O}(1)$ , for instance  $\eta_6 = \mathcal{O}(1)$  and  $\eta_1 = \mathcal{O}(1) > m_h^2/v^2$  [35].

For baryogenesis, we need a complex phase in the Higgs or Yukawa sectors of the general 2HDM. Many analyses have studied a complex Higgs potential, which tends to be strongly constrained by EDM measurements [39–42]. We look at the alternative option of  $CP$ -violation arising from the Yukawa sector [25, 34, 43]

$$\begin{aligned} \mathcal{L} \supset & -\frac{1}{\sqrt{2}} \sum_{F=U,D,L} \bar{F}_i \left[ (-\lambda_{ij}^F s_\gamma + \rho_{ij}^F c_\gamma) h + (\lambda_{ij}^F c_\gamma + \rho_{ij}^F s_\gamma) H - i \operatorname{sgn}(Q_F) \rho_{ij}^F A \right] P_R F_j \\ & - \bar{U}_i \left[ (V \rho^D)_{ij} P_R - (\rho^{U\dagger} V)_{ij} P_L \right] D_j H^+ - \bar{\nu}_i \rho_{ij}^L P_R L_j H^+ + \text{h.c.}, \end{aligned} \quad (6)$$

where  $i, j = 1, 2, 3$  are generation indices,  $P_{L,R} \equiv (1 \mp \gamma_5)/2$ , and  $V$  is the CKM matrix. In flavor space, the fermion fields  $F$  are defined as  $U = (u, c, t)$ ,  $D = (d, s, b)$ ,  $L = (e, \mu, \tau)$  and  $\nu = (\nu_e, \nu_\mu, \nu_\tau)$ . While the mass matrices are diagonalized as in the Standard Model, one cannot rotate away  $CP$ -violating phases of the second set of  $\rho^F$  matrices in the general 2HDM even in the Higgs basis. That is, the two coupling matrices are

$$\lambda_{ij}^F = \sqrt{2} \frac{m_i^F}{v} \delta_{ij} \in \mathbb{R} \quad \text{and} \quad \rho_{ij}^F \in \mathbb{C}. \quad (7)$$

The complex coupling matrices  $\rho^F$  are, strictly speaking, not related to the fermion masses. On the other hand, given experimental constraints and a possible order-of-magnitude correspondence in the values of  $\rho^F$  and  $\lambda^F$  lead us to consider  $\rho_{ij}^U$  or  $\rho_{tt}^U$ .

In principle, a finite imaginary part of  $\rho_{tt}$  can quite robustly drive EWBG [25], which motivates search for channels like  $gg \rightarrow H \rightarrow t\bar{t}$  or  $gg \rightarrow Ht\bar{t} \rightarrow 4t$  [44–46]. We focus instead on complex off-diagonal entries  $\rho_{tj}$ , specifically  $\rho_{tc}$ . With a large phase, this FCNC coupling can also [25] drive EWBG and account for the observed baryon asymmetry if  $\rho_{tt}$  turns out to be small. One merit of the  $\rho_{tc}$  mechanism for EWBG is that  $\rho_{tc}$  does not generate an electron EDM through the Barr-Zee [48] two-loop mechanism, and can therefore more easily [49] evade the ACME bound [50]  $d_e < 1.1 \times 10^{-29}$  e cm. Moreover, as we assumed  $\rho_{ct}$  to be vanishingly small, the constraint on  $\rho_{tc}$  from charm chromo-EDM is also not stringent (see e.g. discussion in Ref. [47]). In particular, for  $|\rho_{tt}| \lesssim 10^{-2}$  the baryon asymmetry can still be generated with [25]

$$|\rho_{tc}| \gtrsim 0.5 \quad \text{and} \quad |c_\gamma| \gtrsim 0.1, \quad (8)$$

assuming a sufficiently large complex phase. We indicate this EWBG-region in Fig. 1, but do not show the masses of the heavier Higgs states, except to remind ourselves that a strong first-order phase transition is possible for [51–60]

$$m_{A,H,H^+} \sim 300 \dots 600 \text{ GeV}. \quad (9)$$

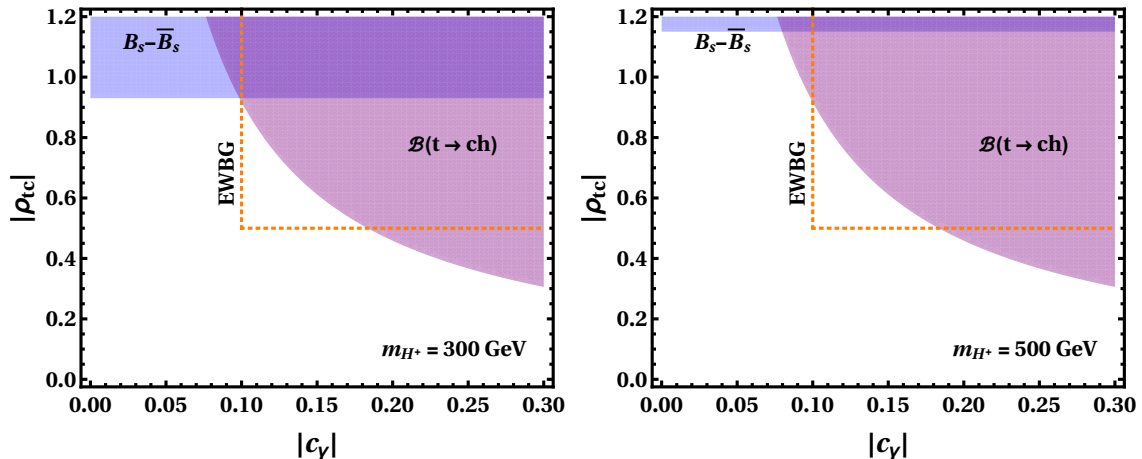


Figure 1: Indirect constraints from  $B_s - \bar{B}_s$  mixing (blue),  $\mathcal{B}(t \rightarrow ch)$  (purple) in the  $\rho_{tc}-c_\gamma$  plane for two  $H^+$  mass values, together with the baryogenesis region (orange).

This mass range, which we will focus on in this paper, is allowed by perturbativity, positivity, unitarity, and electroweak precision data [28, 43, 61–63].

There exist indirect constraints on  $\rho_{tc}$ , which we need to consider before we look at heavy Higgs production at the LHC. For flavor observables,  $\rho_{tc}$  enters through loops with charm quarks and a charged Higgs into  $B_s - \bar{B}_s$  mixing and  $\mathcal{B}(B \rightarrow X_s \gamma)$ . The corresponding limit [64],

$$|\rho_{tc}| \lesssim 1, \quad \text{for } m_{H^+} = 300 \text{ GeV}, \quad (10)$$

is illustrated in Fig. 1. It is relatively weak in our general model, in contrast to the type-II 2HDM. For larger  $m_{H^+}$  values, it rapidly becomes irrelevant.

Moreover, finite  $c_\gamma$  in combination with  $\rho_{tc}$  leads to [20] anomalous top decay  $t \rightarrow ch$  [22], forbidden at tree level in SM. The current Run 2 limits at 95%C.L. are

$$\mathcal{B}(t \rightarrow ch) \approx \frac{c_\gamma^2 |\rho_{tc}|^2}{7.66 + c_\gamma^2 |\rho_{tc}|^2} < \begin{cases} 1.1 \times 10^{-3} & \text{ATLAS [65]} \\ 4.7 \times 10^{-3} & \text{CMS [66]}, \end{cases}$$

which gets weaker for small  $c_\gamma$  and vanishes in the alignment limit. We illustrate the stronger ATLAS [65] constraint also in Fig. 1.

While we will focus on  $\rho_{tc}$  throughout this paper, we point out that  $\rho_{tu}$  can be tested using a very similar strategy. For the LHC processes discussed in the coming sections, there is always a corresponding process with an up-quark replacing the charm-quark. One difference between the two FCNC scenarios is that  $\rho_{tu}$  can induce observable effects in  $\mathcal{B}(B \rightarrow \mu\nu)$  [67], within the reach of Belle-II [68]. The combination of  $\rho_{tc}$  and  $\rho_{tu}$  is subject to very strong constraints from  $D-\bar{D}$  mixing [64], and we will assume only one of the two, but not both at the same time.

### 3 Charged Higgs production

In the EWBG parameter region of Eq.(8), the partonic process at LHC

$$cg \rightarrow bH^+ \rightarrow b(W_\ell^+ h) \rightarrow b W_\ell^+ W_\ell^+ W_\ell^-, \quad (11)$$

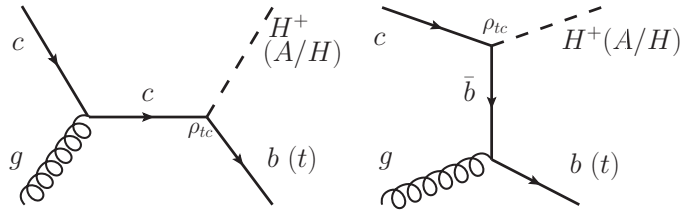


Figure 2: Leading-order Feynman diagrams for the  $\rho_{tc}$ -induced  $cg \rightarrow bH^+$  and  $cg \rightarrow tA/tH$  processes.

probes  $\rho_{tc}$  in  $H^+$ -production and  $c_\gamma$  in  $H^+ \rightarrow W^+h$  decay. The production benefits from the relatively large charm density in the proton, as well as the combination [28] with the CKM matrix element  $V_{tb}$  following Eq.(6). For a clean analysis, we assume that all three  $W$ -bosons decay to either electrons or muons. Strictly speaking, the same process can also be induced by  $\rho_{ct}$ , but this coupling is expected to be much smaller [69] by flavor constraints. The leading-order Feynman diagrams are presented in Fig. 2. While we will require a tagged  $b$ -jet, the  $b$ -inclusive production process could also be defined as  $c\bar{b} \rightarrow H^+$  [70, 71].

The  $H^+W^-h$  coupling, modulated by  $c_\gamma$ , arises from [7, 8]

$$\mathcal{L} \supset -\frac{g_2}{2}c_\gamma (h\partial^\mu H^+ - H^+\partial^\mu h) W_\mu^- + \text{h.c.}, \quad (12)$$

where  $g_2$  is the  $SU(2)$  gauge coupling. To estimate the reach of our charged Higgs signal, we choose two allowed benchmark points,

$$\rho_{tc} = 0.35, \quad c_\gamma = 0.25, \quad m_{H^+} = 350, 500 \text{ GeV}, \quad (13)$$

as given in Tab. 1. For the branching ratios, we ignore the loop-induced decays  $H^+ \rightarrow W^+\gamma$  and  $H^+ \rightarrow W^+Z$ . We generate signal and background events for  $\sqrt{s} = 14$  TeV at leading order with MadGraph5\_aMC@NLO [72]. The effective model is implemented in the FeynRules [73] framework, and for parton densities we use NN23LO1 [74]. The events are showered and hadronized with PYTHIA6.4 [75] and then handed to Delphes3.4.2 [76] for a fast detector simulation with the standard ATLAS card. Jets are reconstructed with an  $R = 0.6$  anti- $k_T$  algorithm [77] in FastJet [78]. For  $b$ -tagging as well as  $c$ -jet and light-jet rejection, we rely on Delphes. To allow for extra jets we apply MLM matching [79, 80]. The signal is generated with up to two additional jets.

The dominant SM-backgrounds are  $t\bar{t}W$  and  $t\bar{t}Z$  production, followed by  $WZ$  + jets,  $4t$ ,  $t\bar{t}h$ ,  $tZj$ ,  $tWZ$ , and  $ZZ$  + jets. Furthermore, we find the backgrounds  $3t$ ,  $3t + W$ , and  $3W$  to be negligible, so we ignore them in our analysis. For background events, we use the same simulation chain as for the signal, with up to one additional jet for  $t\bar{t}W$ ,  $t\bar{t}Z$ ,  $WZ$  + jets,  $ZZ$  + jets, and  $tZ$  + jets, and no QCD jets for the high-multiplicity

$m_{H^+}[\text{GeV}]$	$\Gamma_{H^+}[\text{GeV}]$	$\mathcal{B}(H^+ \rightarrow c\bar{b})$	$\mathcal{B}(H^+ \rightarrow W^+h)$	$\sigma(CG \rightarrow bH^+) [\text{fb}]$
350	2.2	0.85	0.15	0.126
500	3.9	0.66	0.34	0.113

Table 1: Charged Higgs properties for the two benchmark points with  $\rho_{tc} = 0.35$  and  $c_\gamma = 0.25$ . The quoted LHC cross sections include the decay  $H^+ \rightarrow Wh$  in the fully leptonic mode, as shown in Eq.(11), as well as selection and background rejection cuts.

	$t\bar{t}W$	$t\bar{t}\bar{Z}$	$WZ + \text{jets}$	$4t$	$t\bar{t}h$	$tZ + \text{jets}$	$tWZ$	$ZZ + \text{jets}$	sum bkg
merged jets	1	1	1	0	0	1	0	1	
$K$ -factor	NLO	NLO	NNLO	NLO	NLO	NLO	LO	LO	
$\sigma_{\text{bkg}}$ [fb]	0.685	0.279	0.101	0.074	0.026	0.017	0.02	0.001	1.2

Table 2: Background cross sections for the charged Higgs process after cuts.

backgrounds  $4t$ ,  $tWZ$  and  $t\bar{t}h$ . To approximately account for QCD corrections in addition to the jet emission, we attach NLO  $K$ -factors to the dominant  $t\bar{t}V$  backgrounds, namely 1.35 ( $W^-$ ), 1.27 ( $W^+$ ) [81], and 1.56 ( $Z$ ) [82]. We also correct the  $WZ + \text{jets}$  background normalization to NNLO by a factor 2.07 [83]. Furthermore, we adjust the  $4t$ ,  $t\bar{t}h$ , and  $tZ + \text{jets}$  rates to NLO through the  $K$ -factors 2.04 [72], 1.27 [84] and 1.44 [72]. The cross sections for the signal and  $tWZ$  are kept at LO for simplicity. Here, we simply assume the QCD correction factors for the  $W^+Z + \text{jets}$  and  $tZ + \text{jets}$  processes to be the same as their respective charge-conjugate processes.

To suppress the backgrounds, we adopt a simple set of requirements. We start with events containing at least three charged leptons and at least one tagged  $b$ -jet passing

$$\begin{aligned}
p_{T,\ell} &> 20 \text{ GeV}, & |\eta_\ell| &< 2.5, \\
p_{T,b} &> 20 \text{ GeV}, & |\eta_b| &< 2.5, \\
\Delta R_{ij} &> 0.4, & (i, j = \ell, b) \\
\cancel{E}_T &> 35 \text{ GeV}, & m_{\ell+\ell^-} &\not\in [76, 110] \text{ GeV}, \quad (\ell = e, \mu). \quad (14)
\end{aligned}$$

The same-flavor opposite-sign dilepton veto reduces the dominant  $t\bar{t}Z$  background. In case more than one such  $\ell^+\ell^-$  pair exists, we select the combination closest to the  $Z$ -mass for rejection. The remaining signal rate is given in Tab. 1, while the background rates are summarized in Tab. 2.

For discovery reach and exclusion limits, we compute the significance using the likelihood for a simple counting experiment [85]. If we observe  $n$  events with  $n_{\text{pred}}$  predicted, the agreement between observation and prediction is given by

$$Z(n|n_{\text{pred}}) = \sqrt{-2 \ln \frac{L(n|n_{\text{pred}})}{L(n|n)}}, \quad \text{with} \quad L(n|\bar{n}) = \frac{e^{-\bar{n}} \bar{n}^n}{n!}. \quad (15)$$

For discovery, we compare the observed signal plus background with the background prediction and require  $Z(s + b|b) > 5$ . For exclusion, we assume a background-consistent measurement after predicting a signal on top of the background, such that  $Z(b|s + b) > 2$ . For instance, assuming an HL-LHC data set with  $3000 \text{ fb}^{-1}$  and the signal and background cross sections in Tabs. 1 and 2, we find a significance of  $6.6\sigma$  for  $m_{H^+} = 350 \text{ GeV}$  and  $5.9\sigma$  for  $m_{H^+} = 500 \text{ GeV}$ .

We illustrate in Fig. 3 the Run 3 and HL-LHC reach for the charged Higgs signature in the  $|\rho_{tc}|$ - $c_\gamma$  plane. We see from the left panel that Run 3 can exclude  $|\rho_{tc}| > 0.3$  and  $|c_\gamma| = 0.25$  for  $m_{H^\pm} = 350 \text{ GeV}$ , while the HL-LHC will be sensitive to  $|\rho_{tc}| > 0.2$  and  $|c_\gamma| = 0.13$ . For larger Higgs masses, the expected limits become only slightly weaker. The  $b$ -associated charged Higgs channel covers the  $|\rho_{tc}|$  range preferred by EWBG, but there remains a slice of EWBG parameter space with  $|c_\gamma| \lesssim 0.13$ . This follows as an effect of decreasing  $\mathcal{B}(H^\pm \rightarrow W^\pm h)$  with smaller  $c_\gamma$ . Unfortunately, this hole is unlikely to be filled by other charged Higgs decays, because for instance the standard signature  $H^+ \rightarrow t\bar{b}$  requires large production rates.

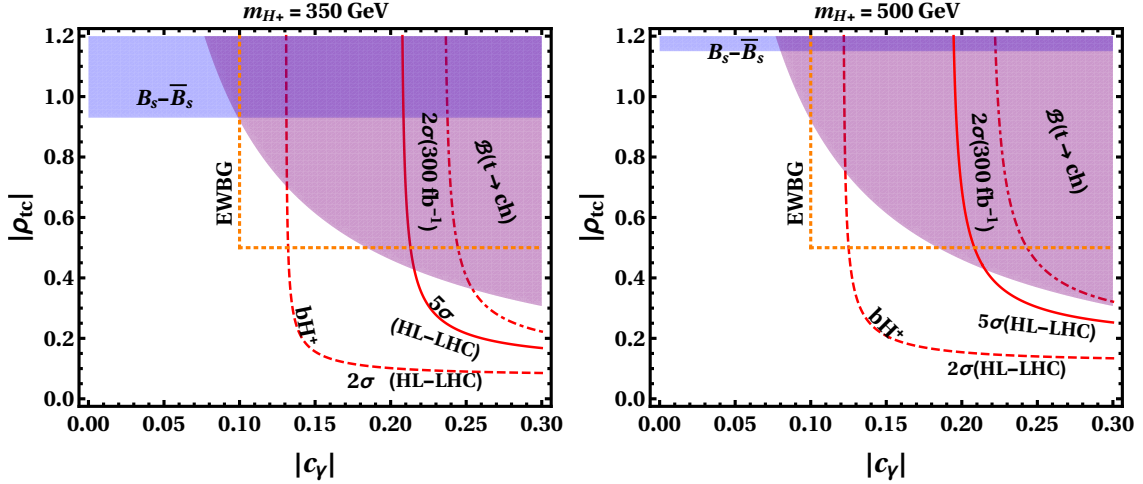


Figure 3: Projected  $300 \text{ fb}^{-1}$  exclusion (dot-dashed) and HL-LHC discovery (solid) and exclusion (dashed) contours for the charged Higgs signature  $pp \rightarrow bH^+ \rightarrow bW^+h$ , along with EWBG-favored region and the indirect constraints from Fig. 1.

## 4 Neutral Higgs production

To cover the parameter region  $|c_\gamma| < 0.13$ , left open by the charged Higgs signature, we turn to the neutral Higgs channel,

$$cg \rightarrow tH/tA \rightarrow t(t\bar{c}), \quad (16)$$

also given in Fig. 2, where the production and decay are both mediated by  $\rho_{tc}$ . A very slight  $c_\gamma$ -dependence of the  $cg \rightarrow tH/tA \rightarrow tt\bar{c}$  process arises from the heavy Higgs branching ratios. Non-resonant and  $t$ -channel diagrams with  $H/A$  exchange leading to  $cc \rightarrow tt$  scattering as well as  $gg \rightarrow tt\bar{c}\bar{c}$ , though small, are included in our signal analysis.

For small  $c_\gamma$ , the neutral Higgs production process currently leads to the most stringent limit on  $\rho_{tc}$  [32,86], because it affects the SM control region of the Run 2  $t\bar{t}t\bar{t}$  ( $4t$ ) analysis by CMS [87]. Based on the number of  $b$ -jets and leptons, CMS divides its analysis into several signal and two control regions. The most stringent constraint on  $\rho_{tc}$  arises from the  $t\bar{t}W$  control region (CRW) [31,32]. The CMS baseline selection includes two same-sign leptons with

$$p_{T,\ell} > 25, 20 \text{ GeV} \quad \text{and} \quad |\eta_e| < 2.5, \quad |\eta_\mu| < 2.4, \quad (17)$$

where the charge-misidentified Drell-Yan background is reduced by vetoing same-sign electron pairs with  $m_{ee} < 12 \text{ GeV}$ . The CRW then requires two to five jets, two of them  $b$ -tagged. All jets have to fulfill  $|\eta_j| < 2.4$ , and events are selected if they fulfill any one of

$$\begin{aligned} \text{(i)} \quad & p_{T,b_1} > 40 \text{ GeV}, \quad p_{T,b_2} > 40 \text{ GeV}, \\ \text{(ii)} \quad & p_{T,b_1} > 20 \text{ GeV}, \quad p_{T,b_2} = 20 \dots 40 \text{ GeV}, \quad p_{T,j_3} > 40 \text{ GeV}, \\ \text{(iii)} \quad & p_{T,b_{1,2}} = 20 \dots 40 \text{ GeV}, \quad p_{T,j_{3,4}} > 40 \text{ GeV}. \end{aligned} \quad (18)$$

Finally, the analysis requires [87]

$$H_T = \sum_{\text{jets}} p_{T,j} > 300 \text{ GeV} \quad \text{and} \quad \cancel{E}_T > 50 \text{ GeV}. \quad (19)$$

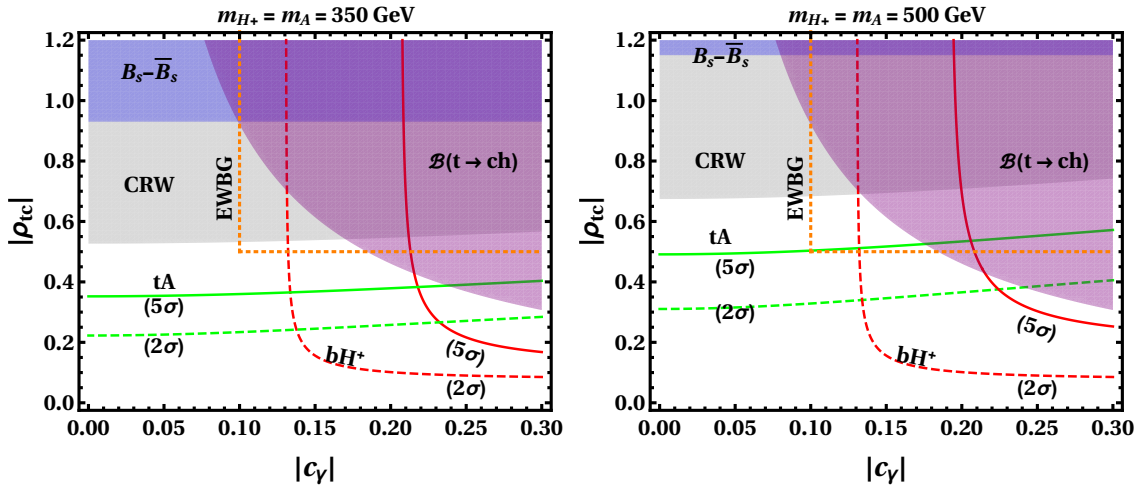


Figure 4: Exclusion regions from neutral Higgs production contributing to the CMS CRW [87] (gray shades), as well as HL-LHC expectations from a dedicated same-sign top search [89] (green). We also show the EWBG region and the indirect constraints from Fig. 1 and the HL-LHC charged Higgs reach from Fig. 3.

With this selection, CMS observes 338 events with  $335 \pm 18$  events expected from SM-backgrounds plus  $4t$  signal. To estimate the CRW limits on  $\rho_{tc}$ , we generate both neutral Higgs processes with the decay  $H/A \rightarrow t\bar{c}$ , followed by lepton-hadron combinations of the top decays at  $\sqrt{s} = 13$  TeV. We use the same setup as for the charged Higgs simulations, except that we use the CMS detector card in Delphes.

There exist a similar ATLAS search [88], but it is less constraining [89]. This is primarily due to the definition of signal regions and selection criteria. Furthermore, searches for squark pair production in  $R$ -parity violating supersymmetry [90] and exotics searches for same-sign dileptons and  $b$ -jets [91] involve similar final states, but their selection cuts are too model-specific to be applied to our signature.

To judge the impact of the existing CMS CRW limits from  $4t$  search, we focus on the border of the EWBG-region with  $c_\gamma = 0.1$  and  $|\rho_{tc}| = 0.5$ . We stick to our two charged Higgs masses, assume  $m_A \approx m_{H^\pm} = 350, 500$  GeV for the pseudoscalar, and decouple the heavy scalar  $H$ . In this scenario, the same-sign top contribution to the CRW arises from  $cg \rightarrow tA \rightarrow tt\bar{c}$ . We demand that the combination of SM-backgrounds and heavy neutral Higgs production agree with observed within  $2\sigma$  and give the excluded regions in Fig. 4. To scan the parameter space we use a simplified scaling  $|\rho_{tc}|^2 \mathcal{B}(A \rightarrow t\bar{c})$ , such that  $\Gamma_A = 3.05$  (6.08) GeV for  $m_A = 350$  (500) GeV. The exclusion covers most of the EWBG-region except for small values of  $|\rho_{tc}|$ . A dedicated same-sign top search [89], summarized in the Appendix, would improve these results [89], and the projected limits are plotted in Fig. 4.

A loop hole in the neutral Higgs analysis appears though the destructive interference of  $cg \rightarrow tH \rightarrow tt\bar{c}$  and  $cg \rightarrow tA \rightarrow tt\bar{c}$ . If the widths and masses of the two heavy neutral Higgses become degenerate, the two production processes completely cancel [31, 32] and the same-sign top signature vanishes. Our limits derived from  $A$ -production would be similar for  $H$ -production with  $m_A \gg m_H$ . We now illustrate limits for  $m_A \sim m_H$  with a case where the three heavy Higgs masses are of similar size, specifically  $m_{H^\pm} = 350$  (500) GeV,  $m_A = 343$  (524) GeV, and  $m_H = 355$  (501) GeV. The self-couplings are  $\eta_1 = 0.276$  (0.297),  $\eta_2 = 1.335$  (2.762),  $\eta_3 = 1.66$  (1.21),  $\eta_4 = -0.04$  (0.398),  $\eta_5 = 0.121$  (-0.428),  $\eta_6 = -0.181$  (-0.386),  $\eta_7 = 0.605$  (-0.095), and  $\mu_{22}^2/v^2 = 1.189$  (3.516), in agreement with

perturbativity, positivity, unitarity, and electroweak precision data [92]. The relevant decays are  $A \rightarrow t\bar{c}$ ,  $Zh$  and  $H \rightarrow t\bar{c}, hh, ZZ, WW$ , with mild contributions from the  $\lambda_f c_\gamma$ -dependent fermionic decays to  $b\bar{b}$  and  $t\bar{t}$ . For  $\rho_{tc} = 0.5$  and  $c_\gamma = 0.1$ , the total widths are  $\Gamma_A = 3.28$  (7.37) GeV and  $\Gamma_H = 2.91$  (6.56) GeV, and the combined contributions to the CRW rates are 0.467 fb and 0.261 fb, corresponding to 64 and 35.8 events. Demanding that the combination of events expected in the SM and from the neutral Higgs channels agree within  $2\sigma$  of the observed number, we find that  $|\rho_{tc}| = 0.5$  is already excluded for  $m_{H^\pm} = 350$  GeV and  $c_\gamma = 0.1$ , and barely allowed for  $m_{H^\pm} = 500$  GeV. We see that, due to the choice of parameters, the cancellation between  $cg \rightarrow tH \rightarrow tt\bar{c}$  and  $cg \rightarrow tA \rightarrow tt\bar{c}$  is not exact, and the CRW limit is stronger than the  $H$  (or  $A$ ) decoupled case.

There exist uncertainties in our results which we have not discussed so far. The  $c$ -initiated processes  $cg \rightarrow bH^+$  and  $cg \rightarrow tA/tH$  have non-negligible systematic uncertainties, such as from parton densities and scale dependence [71, 93–95], which we did not include. Moreover, we do not account for non-prompt and fake backgrounds.

## 5 Outlook

Electroweak baryogenesis is an attractive target for experimental analysis, because it can be tested by a variety of measurements. For any baryogenesis model, it needs to combine new bosonic degrees of freedom with extra  $CP$ -violation. In our case, the new degrees of freedom are provided by a general or type-III 2HDM. If the Higgs self-couplings are sufficiently large, the heavy Higgs states can be relatively heavy, so we use  $m_{H^+} = 350$  and 500 GeV as benchmark scenarios. The complex phase is given by an FCNC top–charm coupling with  $|\rho_{tc}| \gtrsim 0.5$ , combined with a  $CP$ -even Higgs mixing angle  $c_\gamma \gtrsim 0.1$ . At the LHC,  $\rho_{tc}$  has the advantage that we can test it in processes mediated by this large top Yukawa, but with a charm quark in the initial state, while it easily evades the electron EDM constraint.

In the valid 2HDM parameter space, the charged Higgs has to be relatively light, which means we can search for it via  $cg \rightarrow bH^+$  with a subsequent  $H^+ \rightarrow W^+h$  decay. Our proposed analysis is relatively straightforward and probes most of the EWBG parameter space at the HL-LHC, with the exception of small values of  $c_\gamma \sim 0.1 \dots 0.12$ , when  $H^+ \rightarrow W^+h$  decay becomes too suppressed by  $CP$ -even Higgs boson mixing.

A complementary channel that can survive small  $CP$ -even Higgs boson mixing is heavy neutral Higgs production,  $cg \rightarrow tA/tH$ , together with  $A/H \rightarrow t\bar{c}$  decay. In this case, production and decay are both mediated by  $\rho_{tc}$  without being suppressed by small  $c_\gamma$ , providing strong limits on  $\rho_{tc}$  even for small  $c_\gamma$  values. The search channel at the LHC is same-sign top pairs, allowing us to extract limits already from Run 2. In combination, charged and neutral heavy Higgs searches provide a comprehensive coverage of the  $\rho_{tc}$ -driven EWBG parameter space at the HL-LHC, leaving us with the challenge to measure the  $CP$ -violating phase itself assuming discovery.

## Acknowledgments

First, we would like to thank Kai-Feng (Jack) Chen for discussions and for clarifications on Eq.(18). We are also grateful to Eibun Senaha and Margarete Mühleitner for very helpful discussions and comments. WSH is supported by MOST 109-2112-M-002-015-MY3 of Taiwan and NTU 109L104019. TM is supported by a Postdoctoral Research Fellowship

from Alexander von Humboldt Foundation. The research of TP is supported by the Deutsche Forschungsgemeinschaft (German Research Foundation) under grant 396021762 – TRR 257 *Particle Physics Phenomenology after the Higgs Discovery*.

## A Same-sign top study

A dedicated same-sign top search, such as the  $pp \rightarrow tA + X \rightarrow tt\bar{c} + X$  study of Ref. [89], can probe the nominal parameter space of  $\rho_{tc}$ -EWBG. This process can be searched for in events containing same-sign dileptons ( $ee, \mu\mu, e\mu$ ), at least three jets with at least two  $b$ -tag, and some  $\cancel{E}_T$ . The dominant backgrounds are  $t\bar{t}Z$ ,  $t\bar{t}W$ ,  $4t$ , while  $t\bar{t}h$ , with  $tZ + \text{jets}$ ,  $3t + W$  and  $3t + j$  give subdominant contributions, and the non-prompt background can be 1.5 times the rate of  $t\bar{t}W$ . In addition, if a lepton charge gets misidentified, the  $t\bar{t} + \text{jets}$  and  $Z/\gamma^* + \text{jets}$  processes will also contribute. The total background cross sections after selection cuts are summarized in Tab. 3. For further details of the cut-based analysis and QCD correction factors for different backgrounds, we refer to Ref. [89].

For the reference values  $|\rho_{tc}| = 0.5$  and  $c_\gamma = 0.1$ , we generate the same-sign top cross sections for  $m_A = 350$  and  $500$  GeV. Based on the background rates of Tab. 3 and Eq.(15), rescaling the signal cross section by  $|\rho_{tc}|^2 \mathcal{B}(A \rightarrow t\bar{c})$ , we find the exclusion (green dashed) and discovery (green solid) contours in the  $|c_\gamma| - |\rho_{tc}|$  plane as given in Fig. 4.

background	$\sigma$ [fb]	background	$\sigma$ [fb]	background	$\sigma$ [fb]
$t\bar{t}W$	1.31	$t\bar{t}Z$	1.97	$tZ + \text{jets}$	0.007
$4t$	0.092	$3t + W$	0.001	$3t + j$	0.0004
$t\bar{t}h$	0.058	charge-flip	0.024	nonprompt	$1.5 \times t\bar{t}W$

Table 3: Different background cross sections for the dedicated same-sign top search after selection cuts at  $\sqrt{s} = 14$  TeV.

## References

- [1] ATLAS, G. Aad *et al.*, *Observation of a new particle in the search for the Standard Model Higgs boson with the ATLAS detector at the LHC*, Phys. Lett. B **716** (2012) 1, arXiv:1207.7214 [hep-ex].
- [2] CMS, S. Chatrchyan *et al.*, *Observation of a New Boson at a Mass of 125 GeV with the CMS Experiment at the LHC*, Phys. Lett. B **716** (2012) 30, arXiv:1207.7235 [hep-ex].
- [3] A. Biekötter, T. Corbett, and T. Plehn, *The Gauge-Higgs Legacy of the LHC Run II*, SciPost Phys. **6** (2019) 6, 064, arXiv:1812.07587 [hep-ph].
- [4] J. Ellis, C. W. Murphy, V. Sanz, and T. You, *Updated Global SMEFT Fit to Higgs, Diboson and Electroweak Data*, JHEP **06** (2018) 146, arXiv:1803.03252 [hep-ph].
- [5] E. da Silva Almeida, A. Alves, N. Rosa Agostinho, O. J. Éboli, and M. Gonzalez-Garcia, *Electroweak Sector Under Scrutiny: A Combined Analysis of*

- LHC and Electroweak Precision Data*, Phys. Rev. D **99** (2019) 3, 033001, arXiv:1812.01009 [hep-ph].
- [6] T. Lee, *A Theory of Spontaneous T Violation*, Phys. Rev. D **8** (1973) 1226.
- [7] A. Djouadi, *The Anatomy of electro-weak symmetry breaking. I: The Higgs boson in the standard model*, Phys. Rept. **457** (2008) 1, arXiv:hep-ph/0503172.
- [8] G. Branco, P. Ferreira, L. Lavoura, M. Rebelo, M. Sher, and J. P. Silva, *Theory and phenomenology of two-Higgs-doublet models*, Phys. Rept. **516** (2012) 1, arXiv:1106.0034 [hep-ph].
- [9] A. Djouadi, *The Anatomy of electro-weak symmetry breaking. II. The Higgs bosons in the minimal supersymmetric model*, Phys. Rept. **459** (2008) 1, arXiv:hep-ph/0503173.
- [10] C. T. Hill and E. H. Simmons, *Strong Dynamics and Electroweak Symmetry Breaking*, Phys. Rept. **381** (2003) 235, arXiv:hep-ph/0203079. [Erratum: Phys.Rept. 390, 553–554 (2004)].
- [11] M. Schmaltz and D. Tucker-Smith, *Little Higgs review*, Ann. Rev. Nucl. Part. Sci. **55** (2005) 229, arXiv:hep-ph/0502182.
- [12] M. Perelstein, *Little Higgs models and their phenomenology*, Prog. Part. Nucl. Phys. **58** (2007) 247, arXiv:hep-ph/0512128.
- [13] J. C. Pati and A. Salam, *Lepton Number as the Fourth Color*, Phys. Rev. D **10** (1974) 275. [Erratum: Phys.Rev.D 11, 703–703 (1975)].
- [14] F. Gursev, P. Ramond, and P. Sikivie, *A Universal Gauge Theory Model Based on E6*, Phys. Lett. B **60** (1976) 177.
- [15] Y. Achiman and B. Stech, *Quark Lepton Symmetry and Mass Scales in an E6 Unified Gauge Model*, Phys. Lett. B **77** (1978) 389.
- [16] R. Barbieri, D. V. Nanopoulos, and A. Masiero, *Hierarchical Fermion Masses in E6*, Phys. Lett. B **104** (1981) 194.
- [17] A. Sakharov, *Violation of CP Invariance, C asymmetry, and baryon asymmetry of the universe*, Sov. Phys. Usp. **34** (1991) 5, 392.
- [18] A. Bochkarev, S. Kuzmin, and M. Shaposhnikov, *Electroweak baryogenesis and the Higgs boson mass problem*, Phys. Lett. B **244** (1990) 275.
- [19] N. Turok and J. Zadrozny, *Electroweak baryogenesis in the two doublet model*, Nucl. Phys. B **358** (1991) 471.
- [20] K.-F. Chen, W.-S. Hou, C. Kao, and M. Kohda, *When the Higgs meets the Top: Search for  $t \rightarrow ch^0$  at the LHC*, Phys. Lett. **B725** (2013) 378, arXiv:1304.8037 [hep-ph].
- [21] P. Chang, K.-F. Chen, and W.-S. Hou, *Flavor Physics and CP Violation*, Prog. Part. Nucl. Phys. **97** (2017) 261, arXiv:1708.03793 [hep-ph].
- [22] W.-S. Hou, *Tree level  $t \rightarrow ch^0$  or  $h^0 \rightarrow t\bar{c}$  decays*, Phys. Lett. **B296** (1992) 179.

- [23] D. López-Val, T. Plehn, and M. Rauch, *Measuring extended Higgs sectors as a consistent free couplings model*, JHEP **10** (2013) 134, arXiv:1308.1979 [hep-ph].
- [24] J. Haller, A. Hoecker, R. Kogler, K. Mönig, T. Peiffer, and J. Stelzer, *Update of the global electroweak fit and constraints on two-Higgs-doublet models*, Eur. Phys. J. C **78** (2018) 8, 675, arXiv:1803.01853 [hep-ph].
- [25] K. Fuyuto, W.-S. Hou, and E. Senaha, *Electroweak baryogenesis driven by extra top Yukawa couplings*, Phys. Lett. B **776** (2018) 402, arXiv:1705.05034 [hep-ph].
- [26] S. Gori, C. Grojean, A. Juste, and A. Paul, *Heavy Higgs Searches: Flavour Matters*, JHEP **01** (2018) 108, arXiv:1710.03752 [hep-ph].
- [27] S. Iguro and K. Tobe,  *$R(D^{(*)})$  in a general two Higgs doublet model*, Nucl. Phys. B **925** (2017) 560, arXiv:1708.06176 [hep-ph].
- [28] D. K. Ghosh, W.-S. Hou, and T. Modak, *Sub-TeV  $H^+$  Boson Production as Probe of Extra Top Yukawa Couplings*, Phys. Rev. Lett. **125** (2020) 22, 221801, arXiv:1912.10613 [hep-ph].
- [29] W.-S. Hou, G.-L. Lin, C.-Y. Ma, and C. Yuan, *Probing flavor changing neutral Higgs couplings at LHC*, Phys. Lett. B **409** (1997) 344, arXiv:hep-ph/9702260.
- [30] W. Altmannshofer, J. Eby, S. Gori, M. Lotito, M. Martone, and D. Tuckler, *Collider Signatures of Flavorful Higgs Bosons*, Phys. Rev. D **94** (2016) 11, 115032, arXiv:1610.02398 [hep-ph].
- [31] M. Kohda, T. Modak, and W.-S. Hou, *Searching for new scalar bosons via triple-top signature in  $cg \rightarrow tS^0 \rightarrow tt\bar{t}$* , Phys. Lett. B **776** (2018) 379, arXiv:1710.07260 [hep-ph].
- [32] W.-S. Hou, M. Kohda, and T. Modak, *Constraining a Lighter Exotic Scalar via Same-sign Top*, Phys. Lett. B **786** (2018) 212, arXiv:1808.00333 [hep-ph].
- [33] W. Altmannshofer, B. Maddock, and D. Tuckler, *Rare Top Decays as Probes of Flavorful Higgs Bosons*, Phys. Rev. D **100** (2019) 1, 015003, arXiv:1904.10956 [hep-ph].
- [34] S. Davidson and H. E. Haber, *Basis-independent methods for the two-Higgs-doublet model*, Phys. Rev. D **72** (2005) 035004, arXiv:hep-ph/0504050. [Erratum: Phys.Rev.D 72, 099902 (2005)].
- [35] W.-S. Hou and M. Kikuchi, *Approximate Alignment in Two Higgs Doublet Model with Extra Yukawa Couplings*, EPL **123** (2018) 1, 11001, arXiv:1706.07694 [hep-ph].
- [36] P. Basler and M. Mühlleitner, *BSMPT (Beyond the Standard Model Phase Transitions): A tool for the electroweak phase transition in extended Higgs sectors*, Comput. Phys. Commun. **237** (2019) 62, arXiv:1803.02846 [hep-ph].
- [37] P. Basler, M. Mühlleitner, and J. Müller, *Electroweak Phase Transition in Non-Minimal Higgs Sectors*, JHEP **05** (2020) 016, arXiv:1912.10477 [hep-ph].
- [38] P. Basler, M. Mühlleitner, and J. Müller, *BSMPT v2 A Tool for the Electroweak Phase Transition and the Baryon Asymmetry of the Universe in Extended Higgs Sectors*, arXiv:2007.01725 [hep-ph].

- [39] J. M. Cline, K. Kainulainen, and A. P. Vischer, *Dynamics of two Higgs doublet CP violation and baryogenesis at the electroweak phase transition*, Phys. Rev. D **54** (1996) 2451, arXiv:hep-ph/9506284.
- [40] K. Funakubo, A. Kakuto, S. Otsuki, K. Takenaga, and F. Toyoda, *CP violating profile of the electroweak bubble wall*, Prog. Theor. Phys. **94** (1995) 845, arXiv:hep-ph/9507452.
- [41] G. Dorsch, S. Huber, T. Konstandin, and J. No, *A Second Higgs Doublet in the Early Universe: Baryogenesis and Gravitational Waves*, JCAP **05** (2017) 052, arXiv:1611.05874 [hep-ph].
- [42] P. Basler, M. Mühlleitner, and J. Wittbrodt, *The CP-Violating 2HDM in Light of a Strong First Order Electroweak Phase Transition and Implications for Higgs Pair Production*, JHEP **03** (2018) 061, arXiv:1711.04097 [hep-ph].
- [43] W.-S. Hou and T. Modak, *Prospects for  $tZH$  and  $tZh$  production at the LHC*, Phys. Rev. D **101** (2020) 3, 035007, arXiv:1911.06010 [hep-ph].
- [44] N. Craig, F. D’Eramo, P. Draper, S. Thomas, and H. Zhang, *The Hunt for the Rest of the Higgs Bosons*, JHEP **06** (2015) 137, arXiv:1504.04630 [hep-ph].
- [45] S. Kanemura, H. Yokoya, and Y.-J. Zheng, *Searches for additional Higgs bosons in multi-top-quarks events at the LHC and the International Linear Collider*, Nucl. Phys. B **898** (2015) 286, arXiv:1505.01089 [hep-ph].
- [46] S. Gori, I.-W. Kim, N. R. Shah, and K. M. Zurek, *Closing the Wedge: Search Strategies for Extended Higgs Sectors with Heavy Flavor Final States*, Phys. Rev. D **93** (2016) 7, 075038, arXiv:1602.02782 [hep-ph].
- [47] F. Sala, *A bound on the charm chromo-EDM and its implications*, JHEP **03** (2014) 061, arXiv:1312.2589 [hep-ph].
- [48] S. M. Barr and A. Zee, *Electric Dipole Moment of the Electron and of the Neutron*, Phys. Rev. Lett. **65** (1990) 21. [Erratum: Phys. Rev. Lett.65,2920(1990)].
- [49] K. Fuyuto, W.-S. Hou, and E. Senaha, *Cancellation mechanism for the electron electric dipole moment connected with the baryon asymmetry of the Universe*, Phys. Rev. D **101** (2020) 1, 011901, arXiv:1910.12404 [hep-ph].
- [50] ACME, V. Andreev *et al.*, *Improved limit on the electric dipole moment of the electron*, Nature **562** (2018) 7727, 355.
- [51] K. Funakubo, A. Kakuto, and K. Takenaga, *The Effective potential of electroweak theory with two massless Higgs doublets at finite temperature*, Prog. Theor. Phys. **91** (1994) 341, arXiv:hep-ph/9310267.
- [52] J. M. Cline and P.-A. Lemieux, *Electroweak phase transition in two Higgs doublet models*, Phys. Rev. D **55** (1997) 3873, arXiv:hep-ph/9609240.
- [53] S. Kanemura, Y. Okada, and E. Senaha, *Electroweak baryogenesis and quantum corrections to the triple Higgs boson coupling*, Phys. Lett. B **606** (2005) 361, arXiv:hep-ph/0411354.
- [54] L. Fromme, S. J. Huber, and M. Seniuch, *Baryogenesis in the two-Higgs doublet model*, JHEP **11** (2006) 038, arXiv:hep-ph/0605242.

- [55] D. Borah and J. M. Cline, *Inert Doublet Dark Matter with Strong Electroweak Phase Transition*, Phys. Rev. D **86** (2012) 055001, arXiv:1204.4722 [hep-ph].
- [56] J. M. Cline and K. Kainulainen, *Improved Electroweak Phase Transition with Subdominant Inert Doublet Dark Matter*, Phys. Rev. D **87** (2013) 7, 071701, arXiv:1302.2614 [hep-ph].
- [57] G. Dorsch, S. Huber, and J. No, *A strong electroweak phase transition in the 2HDM after LHC8*, JHEP **10** (2013) 029, arXiv:1305.6610 [hep-ph].
- [58] N. Blinov, S. Profumo, and T. Stefaniak, *The Electroweak Phase Transition in the Inert Doublet Model*, JCAP **07** (2015) 028, arXiv:1504.05949 [hep-ph].
- [59] K. Fuyuto and E. Senaha, *Sphaleron and critical bubble in the scale invariant two Higgs doublet model*, Phys. Lett. B **747** (2015) 152, arXiv:1504.04291 [hep-ph].
- [60] P. Basler, M. Krause, M. Muhlleitner, J. Wittbrodt, and A. Wlotzka, *Strong First Order Electroweak Phase Transition in the CP-Conserving 2HDM Revisited*, JHEP **02** (2017) 121, arXiv:1612.04086 [hep-ph].
- [61] W.-S. Hou, M. Kohda, and T. Modak, *Top-assisted di-Higgs boson production motivated by baryogenesis*, Phys. Rev. D **99** (2019) 5, 055046, arXiv:1901.00105 [hep-ph].
- [62] T. Modak, *Probing an additional bottom Yukawa coupling via  $bg \rightarrow bA \rightarrow bZH$  signature*, Phys. Rev. D **100** (2019) 3, 035018, arXiv:1905.02137 [hep-ph].
- [63] T. Modak and E. Senaha, *Probing Electroweak Baryogenesis induced by extra bottom Yukawa coupling via EDMs and collider signatures*, JHEP **11** (2020) 025, arXiv:2005.09928 [hep-ph].
- [64] A. Crivellin, A. Kokulu, and C. Greub, *Flavor-phenomenology of two-Higgs-doublet models with generic Yukawa structure*, Phys. Rev. D **87** (2013) 9, 094031, arXiv:1303.5877 [hep-ph].
- [65] ATLAS, M. Aaboud *et al.*, *Search for top-quark decays  $t \rightarrow Hq$  with  $36 \text{ fb}^{-1}$  of  $pp$  collision data at  $\sqrt{s} = 13 \text{ TeV}$  with the ATLAS detector*, JHEP **05** (2019) 123, arXiv:1812.11568 [hep-ex].
- [66] CMS, A. M. Sirunyan *et al.*, *Search for the flavor-changing neutral current interactions of the top quark and the Higgs boson which decays into a pair of  $b$  quarks at  $\sqrt{s} = 13 \text{ TeV}$* , JHEP **06** (2018) 102, arXiv:1712.02399 [hep-ex].
- [67] W.-S. Hou, M. Kohda, T. Modak, and G.-G. Wong, *Enhanced  $B \rightarrow \mu\bar{\nu}$  decay at tree level as probe of extra Yukawa couplings*, Phys. Lett. B **800** (2020) 135105, arXiv:1903.03016 [hep-ph].
- [68] Belle-II, W. Altmannshofer *et al.*, *The Belle II Physics Book*, PTEP **2019** (2019) 12, 123C01, arXiv:1808.10567 [hep-ex]. [Erratum: PTEP 2020, 029201 (2020)].
- [69] B. Altunkaynak, W.-S. Hou, C. Kao, M. Kohda, and B. McCoy, *Flavor Changing Heavy Higgs Interactions at the LHC*, Phys. Lett. B **751** (2015) 135, arXiv:1506.00651 [hep-ph].
- [70] T. Plehn, *Charged Higgs boson production in bottom gluon fusion*, Phys. Rev. D **67** (2003) 014018, arXiv:hep-ph/0206121.

- [71] E. Boos and T. Plehn, *Higgs boson production induced by bottom quarks*, Phys. Rev. D **69** (2004) 094005, arXiv:hep-ph/0304034.
- [72] J. Alwall, R. Frederix, S. Frixione, V. Hirschi, F. Maltoni, O. Mattelaer, H. S. Shao, T. Stelzer, P. Torrielli, and M. Zaro, *The automated computation of tree-level and next-to-leading order differential cross sections, and their matching to parton shower simulations*, JHEP **07** (2014) 079, arXiv:1405.0301 [hep-ph].
- [73] A. Alloul, N. D. Christensen, C. Degrande, C. Duhr, and B. Fuks, *FeynRules 2.0 - A complete toolbox for tree-level phenomenology*, Comput. Phys. Commun. **185** (2014) 2250, arXiv:1310.1921 [hep-ph].
- [74] NNPDF, R. D. Ball, V. Bertone, S. Carrazza, L. Del Debbio, S. Forte, A. Guffanti, N. P. Hartland, and J. Rojo, *Parton distributions with QED corrections*, Nucl. Phys. B **877** (2013) 290, arXiv:1308.0598 [hep-ph].
- [75] T. Sjostrand, S. Mrenna, and P. Z. Skands, *PYTHIA 6.4 Physics and Manual*, JHEP **05** (2006) 026, arXiv:hep-ph/0603175.
- [76] DELPHES 3, J. de Favereau, C. Delaere, P. Demin, A. Giammanco, V. Lemaître, A. Mertens, and M. Selvaggi, *DELPHES 3, A modular framework for fast simulation of a generic collider experiment*, JHEP **02** (2014) 057, arXiv:1307.6346 [hep-ex].
- [77] M. Cacciari, G. P. Salam, and G. Soyez, *The anti- $k_t$  jet clustering algorithm*, JHEP **04** (2008) 063, arXiv:0802.1189 [hep-ph].
- [78] M. Cacciari, G. P. Salam, and G. Soyez, *FastJet User Manual*, Eur. Phys. J. C **72** (2012) 1896, arXiv:1111.6097 [hep-ph].
- [79] M. L. Mangano, M. Moretti, F. Piccinini, and M. Treccani, *Matching matrix elements and shower evolution for top-quark production in hadronic collisions*, JHEP **01** (2007) 013, arXiv:hep-ph/0611129.
- [80] J. Alwall *et al.*, *Comparative study of various algorithms for the merging of parton showers and matrix elements in hadronic collisions*, Eur. Phys. J. C **53** (2008) 473, arXiv:0706.2569 [hep-ph].
- [81] J. M. Campbell and R. Ellis,  *$t\bar{t}W^{+-}$  production and decay at NLO*, JHEP **07** (2012) 052, arXiv:1204.5678 [hep-ph].
- [82] J. Campbell, R. K. Ellis, and R. Röntsch, *Single top production in association with a Z boson at the LHC*, Phys. Rev. D **87** (2013) 114006, arXiv:1302.3856 [hep-ph].
- [83] M. Grazzini, S. Kallweit, D. Rathlev, and M. Wiesemann,  *$W^{\pm}Z$  production at hadron colliders in NNLO QCD*, Phys. Lett. B **761** (2016) 179, arXiv:1604.08576 [hep-ph].
- [84] “SM Higgs production cross sections at  $\sqrt{s} = 14$  TeV.”.
- [85] G. Cowan, K. Cranmer, E. Gross, and O. Vitells, *Asymptotic formulae for likelihood-based tests of new physics*, Eur. Phys. J. C **71** (2011) 1554, arXiv:1007.1727 [physics.data-an]. [Erratum: Eur.Phys.J.C 73, 2501 (2013)].
- [86] W.-S. Hou, M. Kohda, and T. Modak, *Implications of Four-Top and Top-Pair Studies on Triple-Top Production*, Phys. Lett. B **798** (2019) 134953, arXiv:1906.09703 [hep-ph].

- [87] CMS, A. M. Sirunyan *et al.*, *Search for production of four top quarks in final states with same-sign or multiple leptons in proton-proton collisions at  $\sqrt{s} = 13$  TeV*, Eur. Phys. J. C **80** (2020) 2, 75, arXiv:1908.06463 [hep-ex].
- [88] ATLAS, G. Aad *et al.*, *Evidence for  $t\bar{t}t\bar{t}$  production in the multilepton final state in proton-proton collisions at  $\sqrt{s}=13$  TeV with the ATLAS detector*, Eur. Phys. J. **C80** (2020) 11, 1085, arXiv:2007.14858 [hep-ex].
- [89] W.-S. Hou, T.-H. Hsu, and T. Modak, *Constraining the  $t \rightarrow u$  flavor changing neutral Higgs coupling at the LHC*, Phys. Rev. D **102** (2020) 5, 055006, arXiv:2008.02573 [hep-ph].
- [90] ATLAS, G. Aad *et al.*, *Search for squarks and gluinos in final states with same-sign leptons and jets using  $139 \text{ fb}^{-1}$  of data collected with the ATLAS detector*, JHEP **06** (2020) 046, arXiv:1909.08457 [hep-ex].
- [91] ATLAS, M. Aaboud *et al.*, *Search for new phenomena in events with same-charge leptons and  $b$ -jets in  $pp$  collisions at  $\sqrt{s} = 13$  TeV with the ATLAS detector*, JHEP **12** (2018) 039, arXiv:1807.11883 [hep-ex].
- [92] D. Eriksson, J. Rathsman, and O. Stal, *2HDMC: Two-Higgs-Doublet Model Calculator Physics and Manual*, Comput. Phys. Commun. **181** (2010) 189, arXiv:0902.0851 [hep-ph].
- [93] M. Buza, Y. Matiounine, J. Smith, and W. van Neerven, *Charm electroproduction viewed in the variable flavor number scheme versus fixed order perturbation theory*, Eur. Phys. J. C **1** (1998) 301, arXiv:hep-ph/9612398.
- [94] F. Maltoni, G. Ridolfi, and M. Ubiali,  *$b$ -initiated processes at the LHC: a reappraisal*, JHEP **07** (2012) 022, arXiv:1203.6393 [hep-ph]. [Erratum: JHEP 04, 095 (2013)].
- [95] J. Butterworth *et al.*, *PDF4LHC recommendations for LHC Run II*, J. Phys. G **43** (2016) 023001, arXiv:1510.03865 [hep-ph].